JOURNAL OF MATERIALS SCIENCE 29 (1994) 3724–3732

Effect of Fe content on the mechanical alloying and mechanical properties of Al–Fe alloys

X. P. NIU, L. FROYEN, L. DELAEY
Department of Metallurgy and Material Engineering, Katholieke Universiteit Leuven, de Croylaan 2, B-3001 Leuven, Belgium

C. PEYTOUR
Direction des Etudes Matériaux, Renault, 8-10 Avenue Emile-Zola, F-92109 Boulogne Billancourt, France

Al–Fe alloys with Fe contents ranging from 5 to 12 wt% are produced by a double mechanical alloying process (DMA) which consists of a first step of mechanical alloying (MA1) applied to elemental Al and Fe powders, with subsequent heat treatment of MA1 powders to promote the formation of Al–Fe intermetallic phases, and a second mechanical alloying step (MA2) to refine the intermetallic phase, and consolidation of the produced powders by combination of degassing and hot extrusion. The effect of Fe content on the process, as well as on the mechanical properties of the extruded alloys, has been extensively studied. The alloys produced by this process show excellent tensile strength and stiffness at room and elevated temperatures due to the strengthening of Al by intermetallics, as well as to the stabilization of the structure by inert dispersoids.

1. Introduction

Al alloys have been widely used in the engineering industry because of their attractive properties, such as light weight, high ductility, corrosion resistance and toughness. However, the conventional Al alloys have very poor strength and stiffness at elevated temperatures compared to steel and nickel alloys. Their applications are often restricted to the low temperatures. Therefore, there has been a strong demand for the development of new Al alloys with improved elevated temperatures stability.

Rapid solidification processes (RSP) have been used as a technique for the production of high temperature Al alloys since the 1970s. Among the systems of interest, binary Al–Fe and Al–Fe based alloys with additions of transition elements, or some rare earth elements, via RSP have been extensively studied in the past [1–7]. In the rapid solidification process, extended solid solubility of Fe in Al up to 8.4 wt % can be obtained by suppressing the equilibrium cooling reaction. This results in a final product containing a high volume fraction of precipitate intermetallics with a size of about 1 μm. Possible application temperatures of Al–Fe based alloys have been reported up to 315 °C. However, the properties of these RSP Al–Fe alloys decrease drastically at higher temperatures due to rapid coarsening of intermetallic phases.

Since mechanical alloying (MA) was invented by J. S. Benjamin in the 1960s, it soon became an alternative technique for fabrication of high temperature Al alloys. In an MA process, elemental powders or pre-alloyed powders are subjected to mechanical grinding (ball milling) in order to produce composite powders with controlled microstructures [8]. In the case of Al alloys, inert dispersoids, such as Al_2O_3 and Al_4C_3 are formed during MA. These inert dispersoids, mainly situated at the grain boundaries, can stabilize microstructures at elevated temperatures [9]. A good combination of strength, stiffness and structural stability at elevated temperatures has been obtained in MA Al–Ti, MA Al–Fe and Al–Mn alloys [9–11]. In addition, mechanical alloying also offers an elegant possibility to produce nanocrystalline and amorphous Al–Fe materials [12, 13]. An extension of the solubility limit of Fe in Al, which is far beyond those levels obtained by the rapid solidification technique, is also achieved by MA [14].

Intermetallic phases, such as Al_3Ti, Al_6Mn and $Al_{13}Fe_4$ are hardly formed by direct MA. These intermetallics are usually formed in subsequent thermal processes. As shown in a previous work [15], the distribution of these intermetallics in the final product is not uniform after a single MA step. The size of intermetallic phases ranges from 1 to 10 μm. As a result, the alloys show relatively low mechanical properties. In order to modify the distribution of intermetallics, a new technique, namely double mechanical alloying (DMA), has been developed [16] and has been used to fabricate high temperature Al–Fe alloys [15, 17]. In the DMA technique, there are three main steps:

1. First, a mechanical alloying stage applied to elemental powders (called MA1 hereafter), followed by heat treatment of MA1 powders;
2. second, a mechanical alloying stage of heat treated powders (called MA2 hereafter); and

0022–2461 © *1994 Chapman & Hall*

3. further consolidation of the powders produced by a combination of degassing and hot extrusion.

In the present work, Al–Fe alloys with Fe contents ranging from 5 to 12 wt % Fe are produced by the DMA technique. The effect of Fe content on the behaviour of MA, as well as on the mechanical properties of Al–Fe alloys, is studied with the aim of evaluating them for high temperature applications.

2. Experimental procedure

The composition of the material studied is Al–5% Fe, Al–8% Fe, Al–10% Fe and Al–12% Fe (all weight per cent). Elemental water atomized Al and carbonyl Fe powders are ground in a planetary ball mill (Fritsch Pulverisette 5) with an organic additive which acts as a process control agent (PCA). The mean size of the powders is 110 μm for Al and 4 μm for Fe. Both the grinding balls and the vial of the ball mill are made of hardened chromium steel. The weight ratio of the grinding ball to the powder is 10:1. The loading of the powder is done in air atmosphere. Fig. 1 shows the flow sheet of mechanical alloying with two possible routes of single mechanical alloying (SMA) and double mechanical alloying (DMA). In the present work, the process for each stage has been optimized. The elemental powders are first mechanical alloyed (MA1) for 6 h. The MA1 powders are then heat treated for 5 h at 550 °C in argon to form intermetallic phases. After this treatment, the powders are again mechanically alloyed (MA2) for 6 h. After each stage of processing, microhardness and size, as well as the density of MA powders, are determined in order to study the influence of Fe content on the powder properties. Consolidation of MA powders involves cold compaction, encapsulation in an Al-alloy can, vacuum degassing (1 h, 550 °C) and hot extrusion (extrusion ratio, 1:20; extrusion temperature, 430 °C). The mean size of powders is determined with a laser diffractometer (Coulter LS-100), and microhardness is measured with a Leitz hardness tester under 10 g load. The density of the powders is determined with a gas pycnometer. Formation of intermetallic phases is analysed by X-ray diffraction (XRD) with a Cu source, and by differential scanning calorimetry (DSC). Microstructures of the powders and the extruded materials are studied by light optical microscopy (LOM), by scanning electron microscopy (SEM) and by transmission electron microscopy (TEM). Both SEM and TEM are equipped with a Tracor energy dispersive X-ray analyser (EDX). The hardness (HRB) of the extruded alloys is measured with a Rockwell hardness tester under a 100 Kg load. The tensile properties of the extruded alloys are determined at room and elevated temperatures (up to 400 °C).

3. Results

3.1. Powder processing

Fig. 2 shows the variation in microhardness as a function of Fe content. The microhardness of powders after MA1 does not change very much with increasing Fe content, indicating that the effect of Fe content on microhardness is slight. Heat treatment of MA1 powders slightly reduces the microhardness (about 13% reduction) due to a partial release of cold work energy and to the formation of the coarse intermetallics, $Al_{13}Fe_4$. After MA2, a further increase of microhardness is obtained by refinement of intermetallic phases and strain hardening. Unlike those of MA1 powders, increasing Fe content results in an increased microhardness due to an increasing amount of intermetallics. Fig. 3 shows the variation of powder size as a function of Fe content. It is seen that the mean size of both MA1 and MA2 powders decreases with increasing Fe content. This behaviour is probably due to the high amount of Fe in the MA1 powder or to intermetallic phases in the MA2 powder delaying the tendency of particle welding during milling and resulting in a decreased size. Fig. 4 shows the variation of powder density as a function of Fe content. For comparison, the theoretical values calculated from the rule of mixture (ROM) are also plotted in Fig. 4. The density values for the MA1 powder is calculated based on the density of Fe and Al, while those of the MA2 powder are based on the density of $Al_{13}Fe_4$ and Al. It is seen that the density for both MA1 and MA2 powders increases with increasing Fe content, whereas much higher density is obtained for the MA2 powder. However, the measured density is still lower than the theoretical density for both MA1 and MA2 powders.

Evolution of the microstructures after different processing stages is shown in Fig. 5. Based on energy dispersive X-ray (EDX) and X-ray diffraction (XRD) analysis, the microstructure of the powders can be characterized as follows. In MA1 powders (Fig. 5a), the Al matrix contains a dispersion of pure Fe particles with a typical size of about 4 μm and very fine particles (< 1 μm). During subsequent heat treatment, rather coarse intermetallics, $Al_{13}Fe_4$ (5–10 μm) and fine intermetallics are formed *in situ* (Fig. 5c). After

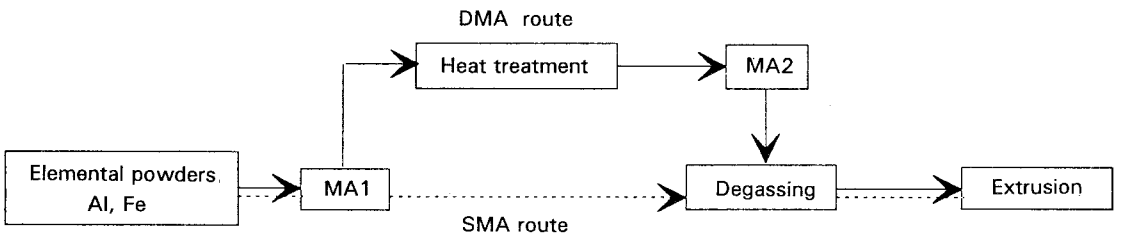

Figure 1 Flow sheet of the mechanical alloying process with two possible routes: (- - - - -) SMA (single mechanical alloying) with one mechanical alloying step (MA1); (——) DMA (double mechanical alloying) with two mechanical alloying steps (MA1 and MA2).

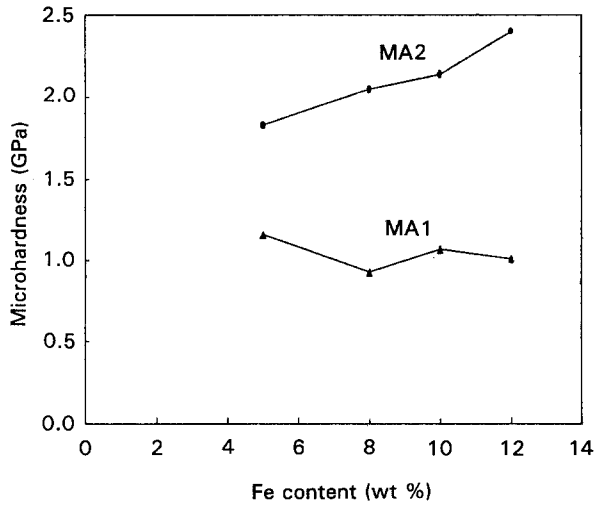

Figure 2 Variation of microhardness with Fe content. MA1, after the first step of mechanical alloying; MA2, after the second step of mechanical alloying.

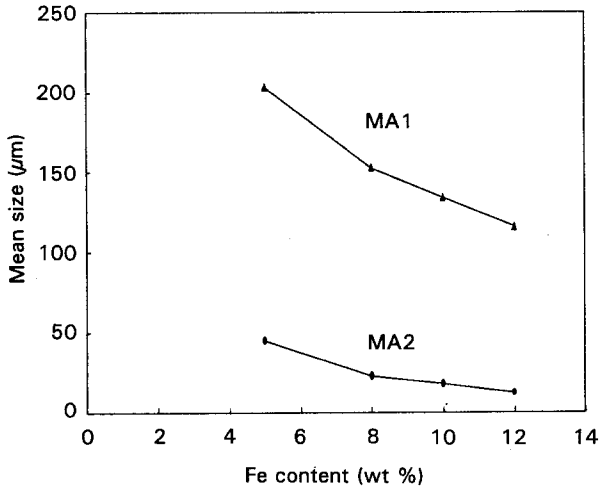

Figure 3 Variation of powder size with Fe content. MA1, after the first step of mechanical alloying; MA2, after the second step of mechanical alloying.

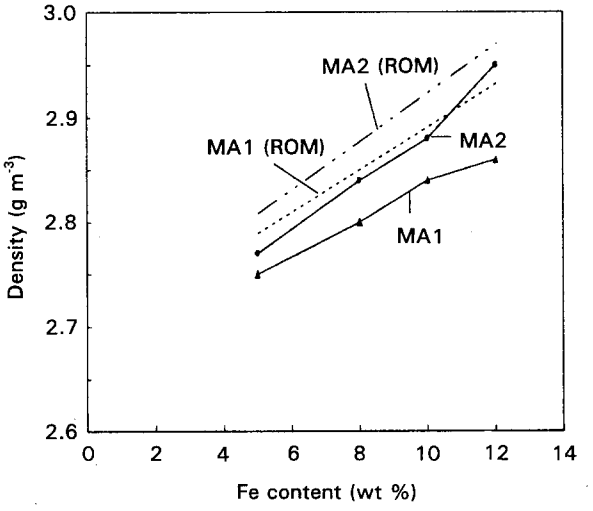

Figure 4 Variation of powder density with Fe content. MA1, after the first step of mechanical alloying; MA2, after the second step of mechanical alloying; MA1(ROM), theoretical value calculated from the rule of mixture based on the density of Fe and Al; MA2 (ROM), theoretical value calculated from the rule of mixture based on the density of $Al_{13}Fe_4$ and Al.

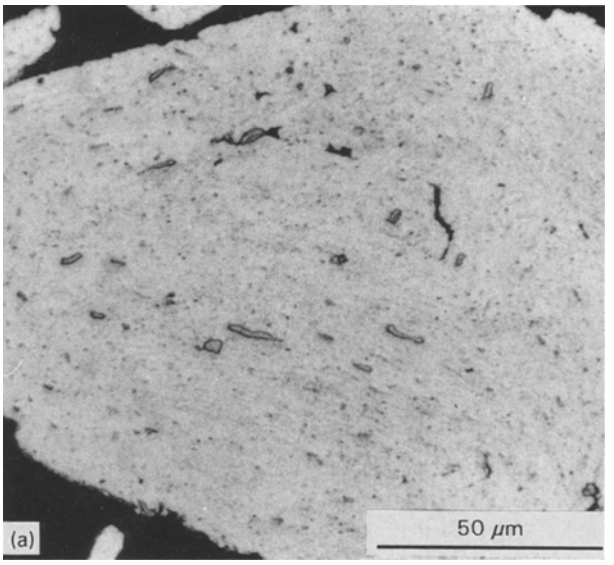

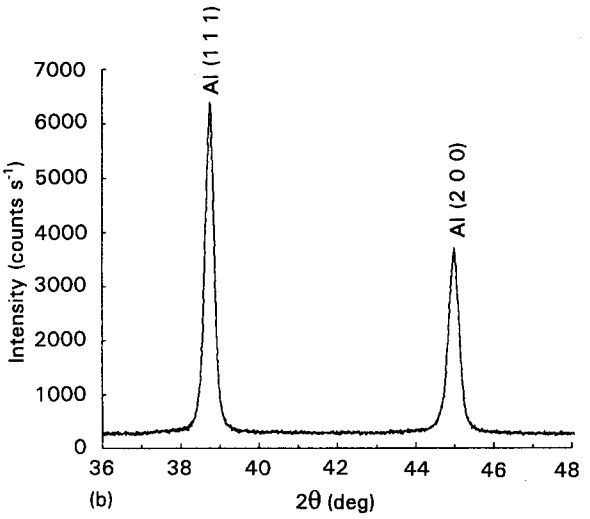

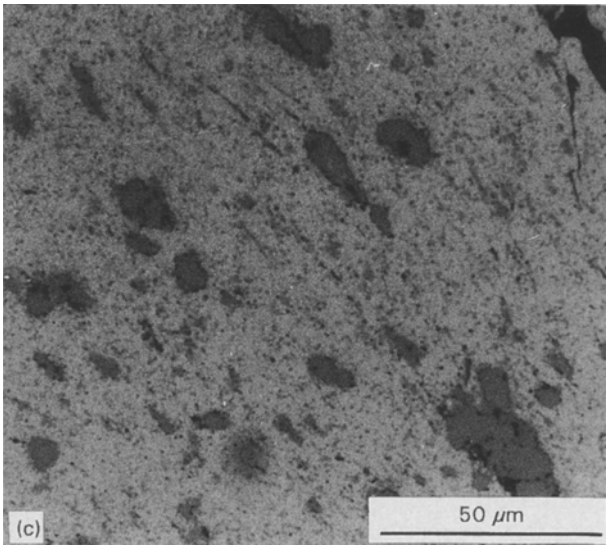

Figure 5 Light optical micrograph of mechanically alloyed powders with X-ray diffraction spectra after different stages: (a, b) MA1 powder, showing the distribution of Fe particles in the Al matrix after the first step of mechanical alloying (Fe cannot be identified in the X-ray diffraction spectrum due to the overlap of peaks between Al and Fe); (c, d) heat-treated powder, showing the formation of the intermetallic phase ($Al_{13}Fe_4$) after heat treatment; and (e, f) MA2 powder, showing the distribution of refined intermetallics after the second step of mechanical alloying.

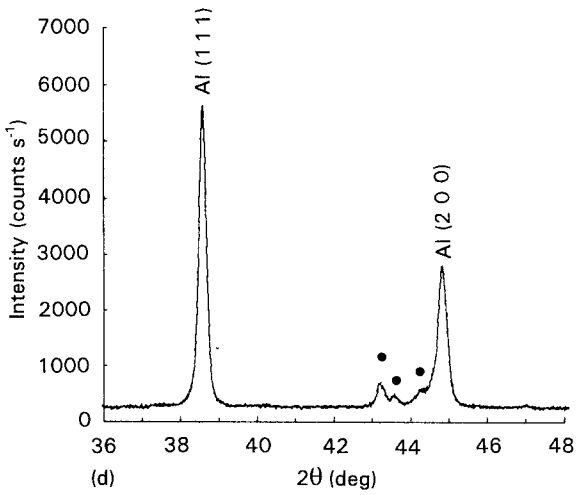

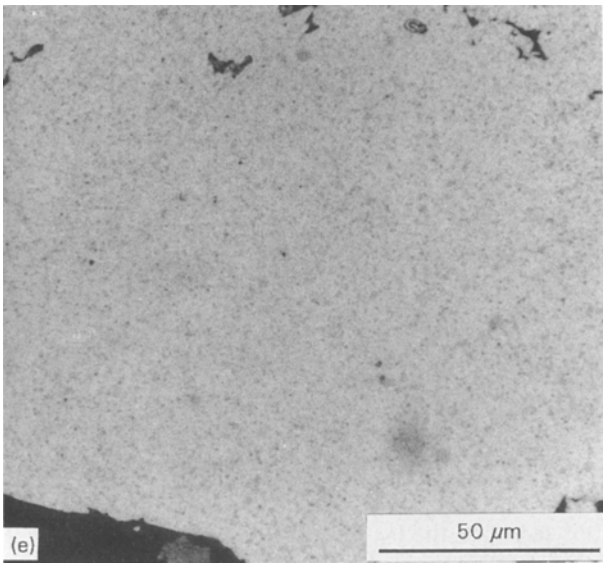

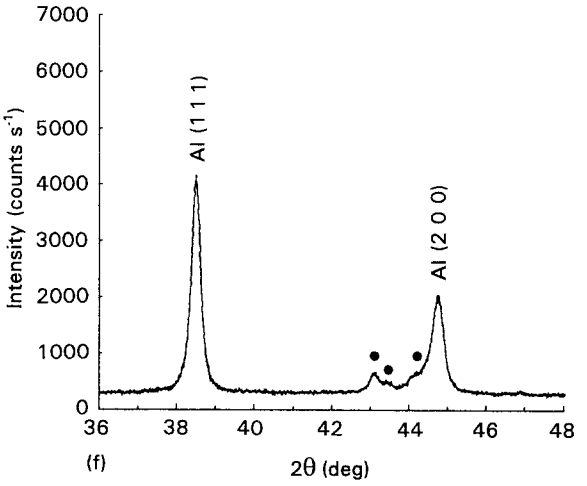

Figure 5 (continued).

MA2, the matrix contains a fine microstructure with a homogeneous distribution of intermetallic phases (Fig. 5e).

As shown in Fig. 5, the intermetallic phases are thus formed during heat treatment of MA1 powder. The kinetics of the reaction between Al and Fe in the MA1 powder has been studied by differential scanning calorimetry (DSC). The reaction order and activation energy for formation of intermetallics can be evaluated based on Kissinger's theory [18]. The variation of the maximum peak temperature, T_m, as a function of heating rate, Φ, is given by

$$\frac{d\ln(\Phi/T_m^2)}{d(1/T_m)} = -\frac{E}{R}$$

where E is the activation energy and R is the gas constant. By plotting $\ln(\Phi/T_m^2)$ as a function of $1/T_m$, a linear relationship has been obtained, if measured at different heating rates. This indicates that the reaction between Al and Fe is kinetically of the first-order. For powders containing 5–12 wt % Fe, the activation energy for the formation of $Al_{13}Fe_4$ comprises between 194 and 201 kJ mol^{-1}.

3.2. Microstructure of the extruded alloys

After powder processing, the produced powders were subjected to consolidation by degassing and hot extrusion. Fig. 6 shows the SEM microstructure of the extruded Al–Fe alloys. It is seen that the intermetallic particles ($Al_{13}Fe_4$) are finely distributed in the Al matrix. The size of most intermetallics ranges from 0.1 to 0.6 μm. Some large intermetallic particles with a size up to 2 μm are present in alloys containing high contents of Fe.

TEM microstructure of the extruded Al–Fe alloy shows the details of the $Al_{13}Fe_4$ phase and Al subgrains (Fig. 7). The extruded alloys have a fine microstructure. The subgrain size of Al ranges from 0.1 to 0.5 μm. The $Al_{13}Fe_4$ phase has a monoclinic structure, with crystal parameters [19] $a = 1.5489$, $b = 0.8083$, $c = 1.2476$ nm and $\beta = 107.71°$. $Al_{13}Fe_4$ often shows a pronounced stacking fault [20]. In the diffraction pattern (Fig. 7), faulting is observed in the [0 1 0] orientation. The line along the 0 0 1 row may be caused by stacking faults on the (0 0 1) plane. Faulting is also observed in other orientations, for example in the [1 1 0]. Aside from that, $Al_{13}Fe_4$ crystals are also frequently observed to be twinned [20].

Mechanical alloying also induces the development of fine scale inert dispersoids, such as Al_4C_3 and Al_2O_3. The size of these inert dispersoids is about 30–40 nm. They are distributed within the matrix, subgrain boundaries or sometimes at the matrix–intermetallic interface.

3.3. Mechanical properties

Mechanical properties of the SMA and DMA Al–5% Fe alloys are summarized in Table I. Fig. 8a–c shows ultimate tensile strength (UTS), E modulus, and elongation as a function of test temperatures and Fe content for the DMA Al–Fe alloys.

The tensile strength and E modulus of Al–5% Fe alloys have been improved significantly by the DMA process (Table I). There is about 100 MPa increase in UTS at room temperature and about 40 MPa increase at 400 °C. The fact that the stiffness (E modulus) of the alloy is improved markedly by the DMA process is of particular interest (from 62 GPa for the SMA Al–5% Fe to 81 GPa for the DMA Al–5% Fe). The improved tensile strength and stiffness can be attributed

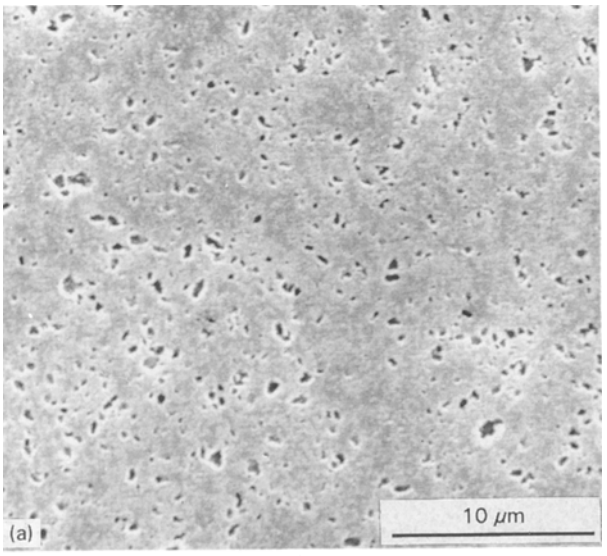

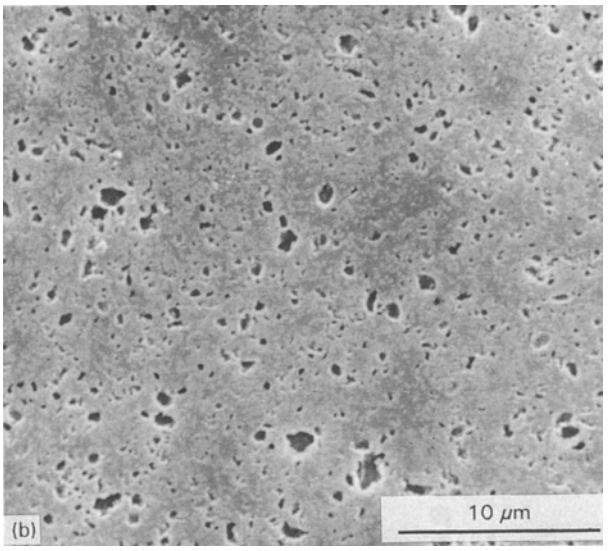

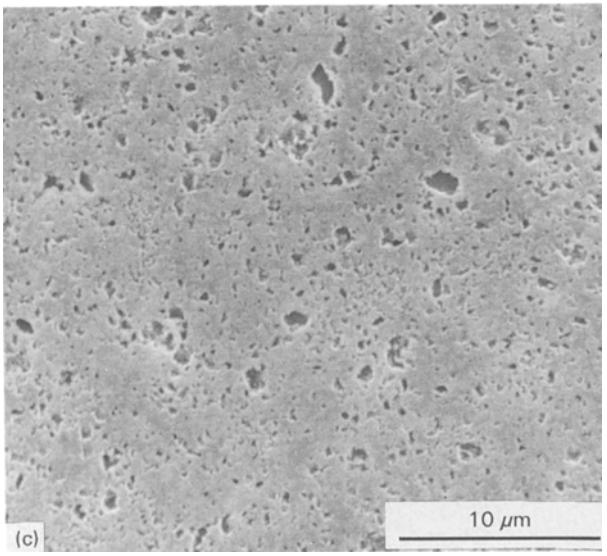

Figure 6 SEM microstructure of the extruded Al–Fe alloys showing the distribution of intermetallic phase $Al_{13}Fe_4$: (a) Al–5% Fe, (b) Al–8% Fe, and (c) Al–12% Fe.

to the homogeneous distribution of intermetallics in the Al matrix by DMA [15]. But, the ductility of the alloy is reduced.

The DMA Al–Fe alloys show a good strength at the temperatures studied (Fig. 8a): more than 450 MPa for UTS and more than 380 MPa for YS are obtained at room temperature. A high level of strength is also maintained at elevated temperatures: more than 180 MPa for both UTS and YS are obtained at 400 °C. It is seen that the Fe content does influence the tensile strength. The strength increases with Fe up to 10 wt % (the maximum strength reaches about 570 MPa). Further increase of Fe to 12 wt % will reduce UTS. At 400 °C, the effect of Fe on the strength is less pronounced.

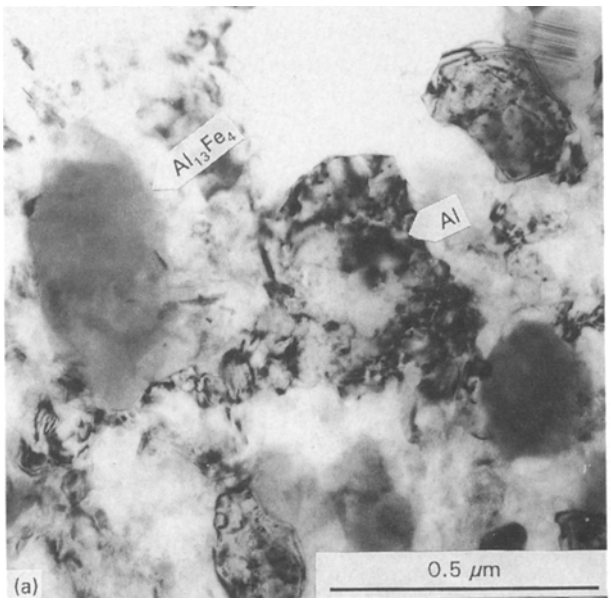

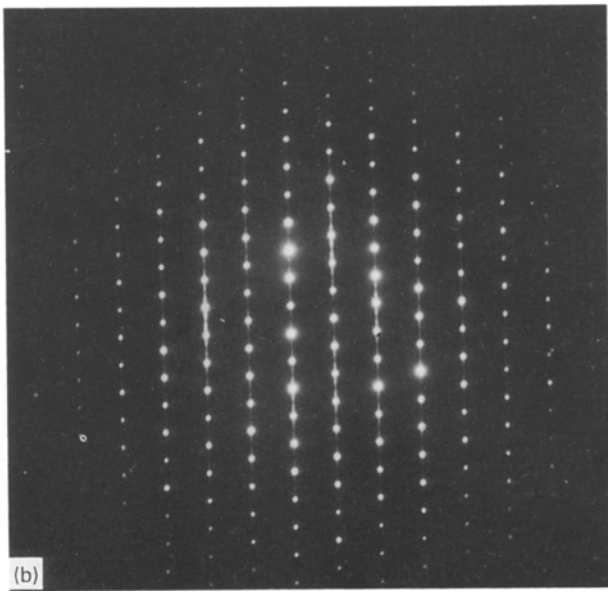

Figure 7 TEM microstructure of the extruded Al–Fe alloy showing (a) the details of $Al_{13}Fe_4$ intermetallic phase and Al subgrains, and (b) the diffraction pattern of $Al_{13}Fe_4$ in the [0 1 0] orientation.

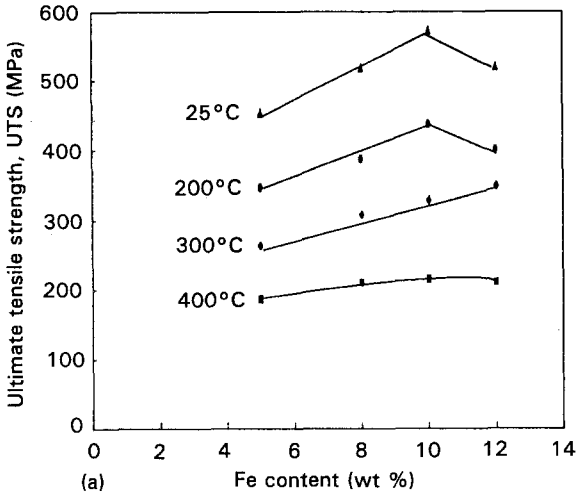

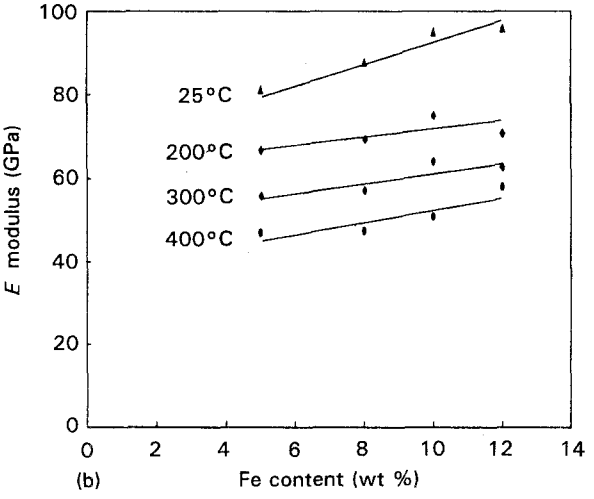

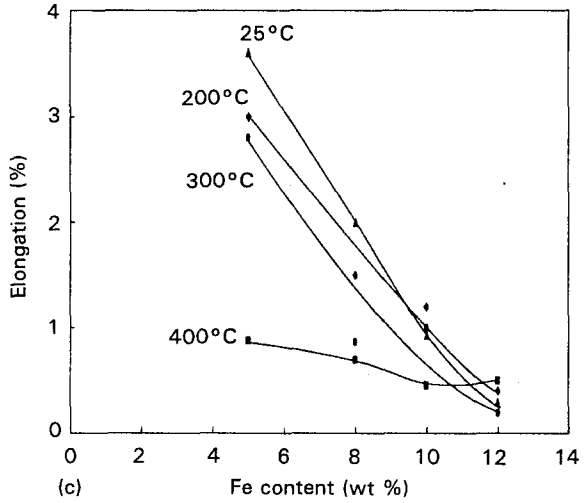

Figure 8 Mechanical properties of the extruded Al–Fe alloys as a function of Fe content: (a) ultimate tensile strength (UTS), (b) E modulus and (c) elongation.

The DMA Al–Fe alloys also show an elevated stiffness (E-modulus) at room temperature as well as at high temperatures. The measured E-modulus ranges from 81 GPa (5 wt % Fe) till 96 GPa (12 wt % Fe) at room temperature, and about 50 GPa at 400 °C. Furthermore, the E modulus increases almost linearly with Fe content. As usual, the E modulus decreases with increasing test temperatures.

The DMA Al–Fe alloys have low ductility. The ductility of the Al–Fe alloys are strongly dependent on the Fe content. Elongation decreases with increasing Fe content and test temperatures. At room temperature, the elongation is less than 4%. At 400 °C, the elongation is less than 1%.

4. Discussion

4.1. Powder processing and formation of intermetallics and inert dispersoids

Mechanical alloying is a process in which repeated fracturing and welding of powders occur throughout the process. The size and microhardness, as well as morphology of the powders, are strongly influenced by the duration of the MA. This behaviour has been revealed in detail elsewhere [15, 17]. In the present work, the effect of Fe on the behaviour of DMA has been investigated. Except for the microhardness of the MA1 powder, microhardness and density of MA powders increase, while the size of MA powders decreases with increasing Fe content. This behaviour can be attributed to the increased amount of intermetallic phases. It has also been observed during the measurement of DSC, that the intensity of the exothermic peak for the formation of $Al_{13}Fe_4$ increases with increasing Fe content, and that the released thermal energy (integral of the peak) also increases. This indicates that more intermetallics are formed with increasing Fe content. With Fe from 5 to 12 wt %, the estimated volume fraction of intermetallics ranges from about 9 to 23 vol %.

In a detailed study of the reaction between Al and Fe in MA Al–25 wt % Fe, it was revealed that a metastable phase, Al_6Fe, was formed prior to the formation of the equilibrium phase $Al_{13}Fe_4$ during

TABLE I Mechanical properties of SMA and DMA Al–5% Fe alloys

Alloy	Test temperature (°C)	σ_{UTS} (MPa)	$\sigma_{0.2}$ (MPa)	E (GPa)	δ (%)	HRB
	25	342.0	302.0	62.0	8.80	55
SMA Al–5%Fe	200	257.0	242.0	49.0	4.60	
	300	222.0	208.0	36.2	4.60	
	400	144.0	144.0	33.0	2.70	
	25	454.0	381.0	81.0	3.60	79
DMA Al–5% Fe	200	347.0	316.0	66.6	2.80	
	300	264.3	250.0	56.0	3.00	
	400	186.3	182.3	47.0	0.88	

heating of the powders [16]. This metastable phase is also observed in the present work by XRD measurement of MA1 powders at 320 °C. With increasing annealing temperature, this metastable phase is eventually transformed into the equilibrium phase, $Al_{13}Fe_4$. From Kissinger's approach, the activation energy for formation of the $Al_{13}Fe_4$ phase obtained in the present work ranges from 194 to 201 kJ mol^{-1}. This value is similar to the activation energy for Fe tracer diffusion in Al (193–256 kJ mol^{-1}) [21], suggesting that formation of the Al–Fe intermetallic phase is controlled by diffusion of Fe through the Al matrix.

The presence of fine scale inert dispersoids (Al_4C_3 and Al_2O_3) in the alloys developed in the present work is the key to improved high temperature properties. Al_4C_3 is formed from the carbon introduced through the PCA. The total content of carbon is about 2.3 wt % after processing. In the course of heat treatment and consolidation, carbon transforms into Al_4C_3. The volume content is estimated to be about 9 vol %. Oxygen is also introduced by the PCA, by the natural oxide layer surrounding the Al powder, and by the air induced in the mill. The content of oxygen is about 1 wt % after milling. The volume content of Al_2O_3 reaches about 2 vol %. Altogether, about 11 vol % of the inert dispersoids, with a size about 30–40 nm, are finally distributed in the alloy.

4.2. Strength and stability

The alloys show an elevated tensile strength both at room temperature and at high temperatures. This improved strength can be virtually attributed to strengthening by intermetallic phases. However, a linear relationship between tensile strength and the volume fraction of intermetallics is not observed in the present work. A further increase in the content of intermetallics from about 18–23 vol % (from 10 to 12 wt % Fe) reduces the tensile strength (from 572 to 520 MPa as shown in Fig. 8a). The material also shows very low ductility. Based on this result, it can be concluded that the Fe content should be less than 10 wt %, which corresponds to the volume fraction of intermetallics, i.e. about 18%. The actual Fe content depends on the applications.

The long term stability is evaluated by a tensile test of the Al–5% Fe alloy after 100 h exposure at 150, 250 and 350 °C. The tensile test is carried out at the same temperature. Fig. 9 shows a comparison of tensile strength between as-extruded and annealed alloys. It is seen that long term annealing does not reduce the strength level, proving that the alloys exhibit good thermal stability. Although the size of intermetallics in the alloys developed in the present work (0.1–0.6 μm) is larger than the size in rapidly solidified Al–Fe alloys (0.02–0.4 μm) [22], the coarsening of the intermetallics during long term exposure at high temperatures was found to be inhibited in the DMA Al–Fe alloys. The presence of fine scale inert dispersoids in the MA alloys are considered to hold the key to enhanced microstructual stability. These dispersoids at the matrix–intermetallics interface may act as a barrier to diffusion of Fe, which is necessary for coarsening [23],

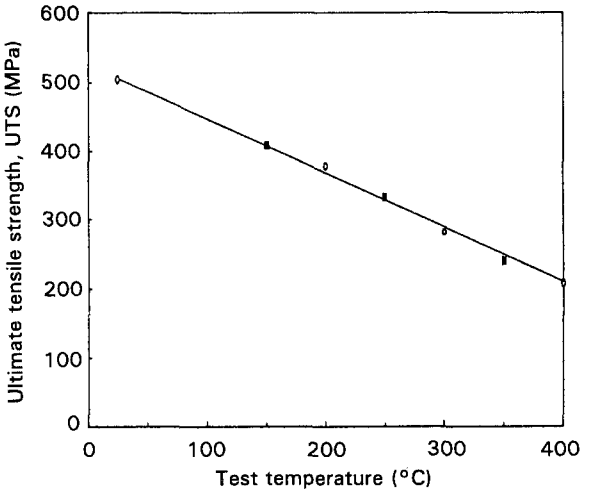

Figure 9 Comparison of the tensile strength between (○) as-extruded and (■) annealed for 100 h Al–5% Fe alloys at various temperatures.

and dispersoids at subgrain boundaries may also act either to pin the subgrain boundaries or further to inhibit diffusion along the boundaries. In fact, even after 100 h exposure at temperatures up to 500 °C there is no drastic change in the microstructure of DMA Al–Fe alloys, except for a slight coarsening of some intermetallics. The subgrain size of Al is still $\leqslant 0.5$ μm. In order to evaluate the mechanical properties of MA Al–Fe alloys, the tensile strength of MA Al–8% Fe alloy is compared to those of RSP Al–Fe alloys [3, 22] (Fig. 10). As seen from this graph, the MA alloy has superior tensile strength to RSP alloys, particularly at elevated temperatures. High temperature strength and good thermal stability of the DMA Al–8% Fe alloy can be attributed to the presence of fine scale inert dispersoids which stabilize the structure at high temperatures. This is an important difference between MA alloys and RSP alloys. The coarsening of intermetallic phases in rapidly solidified Al alloys which are absent from the fine scale inert dispersoids is a main reason for the reduced high temperature properties [23].

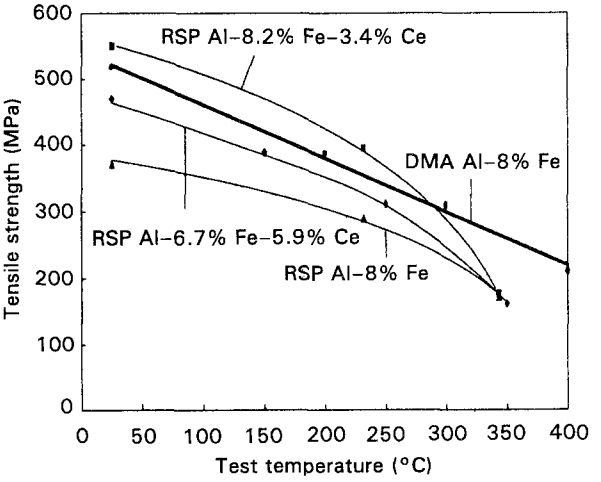

Figure 10 Comparison of the tensile strength at various temperatures between mechanically alloyed Al–8% Fe alloy and rapidly solidified Al–Fe alloys [3, 22].

4.3. Stiffness

Fe is commonly considered as an impurity in conventional Al alloys. In the present work, addition of Fe generates intermetallic phases stable at high temperatures and with a high stiffness (E modulus); they should act as dispersoids and strengthen the Al alloys. As seen before, the stable intermetallic phase formed in the alloys is $Al_{13}Fe_4$. The $Al_{13}Fe_4$ phase has a higher E modulus, 130 GPa [24] compared with that of Al (66–70 GPa). Therefore, the stiffness of Al alloys is expected to be improved by incorporation of such intermetallics. An elevated E modulus is indeed obtained in the alloys developed in the present work. The measured E modulus increases with increasing volume fraction of intermetallics. When the volume fraction of intermetallics varies from 9 to 23%, the values of the E modulus at room temperature range from 81 to 96 GPa. Compared to RSP Al–8% Fe alloy [1], MA Al–8% Fe alloy also shows superior stiffness at both room temperature and elevated temperatures.

In order to evaluate the stiffness of MA Al–Fe alloys, the experimental values are compared with the theoretical values calculated from the theory of lower and upper bounds (LB and UB) [25], and the model of Dudzinski [26] says that E modulus of Al increases linearly with Fe content by 1.58 GPa per wt % Fe. The results are summarized in Fig. 11. It is seen that the measured E modulus of MA Al–Fe alloys is higher than the theoretical values. This excess value may result from inert dispersoids (Al_2O_3 and Al_4C_3). The volume fraction of inert dispersoids in MA Al–Fe alloys is estimated to be about 11 vol %. By comparison between SMA and DMA (Table I), it was shown that the stiffness of the alloys can be effectively improved by modifying the distribution of intermetallic particles through a DMA process.

4.4. Ductility

The main disadvantage of MA Al–Fe alloys is their low ductility. In the present work, elongation of MA Al–Fe alloys is less than 4% at room temperature and less than 1% at 400 °C. The reason for the low ductility of MA Al alloys has been explained elsewhere [15, 17]. First of all the presence of a high volume fraction of hard intermetallic particles limits plastic deformation during the tensile test, causing formation of cracks at the interface between the intermetallic particles and the matrix. This has been observed by examination of the microstructure of the fractured subsurface. Second, inert dispersoids situated at the subgrain boundary can also serve as sites for nucleation of cavities, also reducing the ductility. Finally, high strain hardening in the MA2 powder is also responsible for the low ductility of the extruded alloys. Therefore, strengthening of Al with a high content of intermetallics and inert dispersoids is gained at the expense of ductility.

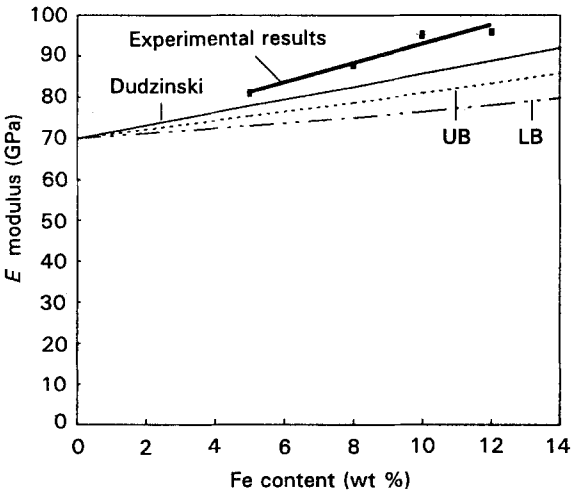

Figure 11 Comparsion of the measured E-modulus with the theoretical Fe values: (UB) upper bounds, (LB) lower bounds.

5. Conclusions

Al–Fe alloys with Fe ranging from 5 to 12 wt % are produced by using a double mechanical alloying process (DMA), containing a first step of mechanical alloying with subsequent heat treatment, a second step of mechanical alloying, and consolidation of the powders involving degassing and hot extrusion.

The behaviour of mechanical alloying and microstructural evolution during the process have been extensively studied. The powder after the first mechanical alloying stage contains Fe particles embedded in the Al matrix. Intermetallic phase $Al_{13}Fe_4$, with a size ranging from 5 to 10 μm, is formed by subsequent heat treatment at high temperatures. Powder containing a fine distribution of intermetallic particles is obtained by the second mechanical alloying stage. The powder properties, such as microhardness, density and size, show a dependence on Fe content during processing. This effect is mainly shown in the second step of mechanical alloying. With increasing Fe content, microhardness and density increase, whereas the size decreases due to an increasing content of intermetallics in the powders.

Compared to single mechanical alloying (SMA), double mechanical alloying (DMA) results in a good combination of strength, stiffness and thermal stability. The extruded alloys show good strength and stiffness at room temperature as well as at elevated temperatures. The effect of Fe content on the mechanical properties exhibits different behaviours. At room temperature, the tensile strength increases initially with Fe content, whereas at much higher Fe (> 10 wt %) the strength will decrease. The stiffness of the alloys increases almost linearly with Fe content. At high temperatures, the effect of Fe on the tensile strength as well as on the stiffness is not significant. The ductility of the material decreases strongly with increasing Fe content and test temperatures. A high Fe content causes rather low ductility. Based on the results, the optimized Fe content in DMA Al–Fe alloys should not exceed 10 wt %.

Improved strength and stiffness at elevated temperatures compared to rapidly solidified alloys are due to the presence of fine scale inert dispersoids (Al_4C_3 and Al_2O_3) which stabilize the structures at high temperatures.

Acknowledgements

The authors would like to thank M. A. Bartet (Renault, France) for performing the tensile tests and A. Jokinen (VTT, Finland) for performing the extrusion. The financial support from Renault, France and the scholarship for X. P. Niu via the Department of MTM, K. U. Leuven are gratefully acknowledged.

References

1. G. THURSFIELD and M. J. STOWELL, *J. Mater. Sci.* **9** (1974) 1644
2. M. H. JACOBS, A. G. DOGGETT and M. J. STOWELL, *ibid.* **9** (1974) 1631.
3. J. R. PICKENS, *ibid.* **16** (1981) 1437.
4. M. A. ZAIDI, J. S. ROBINSON and T. SHEPPARD, *Mater. Sci. Technol.* **1** (1985) 737.
5. C. S. SIVARAMAKRISHNAN, K. LAL and R. K. MAHANTI, *J. Mater. Sci.* **26** (1991) 4369.
6. Y.-W. KIM, in "Proceedings of Dispersion Strengthened Al Alloys, Phoenix, Arizona, January 1988", edited by Y.-W. Kim and W. M. Griffith (The Minerals, Metals & Materials Society, Warrendale, 1988) p. 157.
7. G. M. PHARR, M. S. ZEDALIS, D. J. SKINNER and P. S. GILMAN (The Minerals, Metals & Materials Society, Warrendale, 1988) p. 309.
8. P. S. GILMAN and J. S. BENJAMIN, *Ann. Rev. Mater. Sci.* **13** (1983) 279.
9. J. A. HAWK, P. K. MIRCHANDAN, R. C. BENN and H. G. F. WILSDORF, in "Proceedings of Dispersion Strengthened Al Alloys, Phoenix, Arizona, January 1988", edited by Y.-W. Kim and W. M. Griffth (The Minerals, Metals & Materials Society, Warrendale, 1988) p. 517.
10. P. LE BRUN, X. P. NIU, L. FROYEN, B. MUNAR and L. DELAEY, in "Proceedings of Solid State Powder Processing, Indianapolis, October 1989", edited by A. H. Clauer and J. J. deBarbadillo (The Minerals, Metals & Materials Society, Warrendale, 1990) p. 273.
11. P. LE BURN, L. FROYEN and L. DELAEY, in "Proceedings of Structural Applications of Mechanical Alloying, Mytle Beach, South Carolina, March 1990", edited by F. H. Froes and J. J. deBarbadillo (American Society for Minerals International, 1990) p. 155.
12. P. H. SHINGU, B. HUANG, S. R. NISHITANI and S. NASU, *Trans. JIM* **29** (1988) 3.
13. Y. D. DONG, W. H. WANG, L. LIU, K. Q. XIAO, S. H. TONG and Y. Z. HE, *Mater. Sci. Eng.* **A134** (1991) 867.
14. F. H. FROES and C. SURYANARAYANA, *Int. J. Powder Metall.* April **28/2** (1992) 202.
15. X. P. NIU, P. LE BRUN, L. FROYEN, C. PEYTOUR and L. DELAEY, in "Proceedings of Advances in Powder Metallurgy & Particulate Materials, San Francisco, June 1992", Vol. 7, edited by J. M. Capus and R. M. German (Metal Powder Industries Federation & American Powder Metallurgy Institute, Princeton, 1992) p. 272.
16. P. LE BRUN, L. FROYEN and L. DELAEY, *Mater. Sci. Eng.* **A157** (1992) 79.
17. X. P. NIU, P. LE BRUN, L. FROYEN, C. PEYTOUR and L. DELAEY, *Powder Metall. Int.* **3** (1993) 118.
18. H. E. KISSINGER, *J. Res. National Bureau of Standards* **57** (1956) 217.
19. Powder Diffraction File, PDF-2 data base, Sets 1-40, CD-ROM (International Centre for Diffraction Data, Swarthmore, 1991).
20. P. SKJEPPE, *Metallurg. Trans. A* **18A** (1987) 189.
21. G. RIONTINO, C. ANTONIONE, L. BATTEZZATI and A. ZANADA, *Mater. Sci. Eng.* **A134** (1991) 1166.
22. K. N. RAMAKRISHNAN, H. B. McSHANE and T. SHEPPARD, *Mater. Sci. Technol.* **9** (1993) 104.
23. S. EZZ, M. J. KOCZAK, A. LAWLEY and M. K. PREMKUMAR, in "Proceedings of High Strength Powder Metallurgy Aluminium Alloys II", edited by G. J. Hildeman and M. J. Koczak (The Metallurgical Society, Inc., Warrendale, 1986) p. 287.
24. D. J. SKINNER and M. ZEDALIS, *Scripta Metall.* **22** (1988) 1783.
25. B. PAUL, *Trans. Metall. Soc. AIME* **218** (1960) 36.
26. N. DUDZINSKI, *J. Inst. Metals* **81** (1952–53) 49.

Received 22 June 1993
and accepted 28 January 1994